Effect of oxygen excess ratio on the performance of a hybrid fuel cell system

Ali Moslehi
Department of Mechanical Engineering
University of Quebec in Trois-Rivières
Quebec, Canada
ali.moslehi@uqtr.ca

Mohsen Kandidayeni
Department of Electrical and Computer Engineering
University of Quebec in Trois-Rivières
Quebec, Canada
mohsen.kandi.dayeni@uqtr.ca

Marie Hébert
Department of Mechanical Engineering
University of Quebec in Trois-Rivières
Quebec, Canada
marie.hebert@uqtr.ca

Sousso Kelouwani
Department of Mechanical Engineering
University of Quebec in Trois-Rivières
Quebec, Canada
sousso.kelouwani@uqtr.ca

***Abstract*— This paper considers the significant impact of the oxygen excess ratio (OER) on the hydrogen consumption of a hybrid fuel cell (FC) system. To do so, firstly, a hybrid FC system, composed of an FC stack and a battery pack, is developed in a simulation environment. Subsequently, sequential quadratic programming (SQP), as an optimization-based energy management strategy (EMS), is utilized to minimize hydrogen consumption while respecting the operating constraints of the power sources. Herein, the primary objective is to evaluate the contribution of the OER to the improvement of the FC performance. In this respect, the EMS is equipped with an optimal OER tracker, and its performance is compared with the case where the OER is constant. The results of this study indicate that following an optimal trajectory of OER reduces the hydrogen consumption by nearly 3% under a standard mission profile at sea level conditions.**

Keywords—Energy management strategy, SQP, Hydrogen consumption, Hybrid fuel cell system, Oxygen excess ratio

I. Introduction

The accumulation of carbon dioxide and other greenhouse gases is leading to an increase in the average temperature of the climate system, commonly referred to as global warming. The transportation sector has a significant contribution to the anthropogenic emission of these gases [1].

The adoption of fully electric or hybrid electric vehicle (HEV) technologies is being explored as a potential solution for reducing carbon emissions from traditional vehicles run by fossil fuels. However, owing to drawbacks like restricted driving range and slow recharging rates associated with fully electric vehicles, opting for HEVs emerges as a more viable solution [2]. Similarly, dependence on fossil fuels in HEVs has given rise to alternative sources, including proton exchange membrane (PEM) fuel cells (FCs) in HEVs [3]. These vehicles utilize FC stack as the primary power source, and a battery pack as a secondary power source.

The FC stack is equipped with various auxiliary components, including a compressor, cooling, and hydrogen supply systems, etc. The auxiliary component consuming the most energy is the air compressor. Thus, efficiency improvement efforts focus on compressor. The power consumption of the other auxiliary components is comparatively less significant [4].

To improve the efficiency of a FC system and consequently reduce the operating costs, it is crucial for all components to operate close to their optimal conditions. The air supply plays a crucial role in enhancing system efficiency. Insufficient air supply can result in oxygen starvation, leading to membrane drying, overheating, and potentially irreversible damage to the PEM. Furthermore, temporary voltage fluctuations caused by air starvation, potentially leading to the degradation of cell materials [5]. Conversely, excessive air supply can introduce unnecessary parasitic losses, diminishing system efficiency. The accurate regulation of oxygen excess ratio (OER) can increase the system efficiency significantly [6].

On the other hand, efficient power distribution for a hybrid system is an important issue. An appropriate energy management among power sources can enhance fuel economy of the system [7].

The energy management strategies (EMSs) for HEVs can be categorized into two main types: rule-based, and optimization-based [8]. EMSs based on optimization offer solutions that are close to optimal and have the capability to generate revised guidelines for updating sets of rules and inferential knowledge employed in rule-based approaches [7]. The Sequential Quadratic Programming (SQP) algorithm is one of the most popular methods for solving convex optimization problems and has proven to be efficient for power distribution in hybrid FC systems [9].

In this paper, the optimum OER at each current level is calculated online and the formulation of an EMS with respect to hydrogen consumption of the FC is proposed. The EMS runs once with a constant OER and another time with the optimal value. The results of the two methods are compared under a standard driving cycle.

The remainder of this paper is as follows. Section II describes the FC modeling along with the characteristics of the employed power sources. In section III, a steady state analysis has been done. Section IV deals with the development of the EMS. Section V gives an account of the obtained results of the work, and finally the main conclusions from the performed study are drawn in Section VI.

II. Modeling of Fuel Cell System

Several auxiliary components must be integrated with a FC stack to form a complete FC system. An illustration of a FC system is presented in Fig. 1. An air supply system, hydrogen supply system, cooling system, and humidification system,

alongside the stack are the primary components of a PEMFC power generation system.

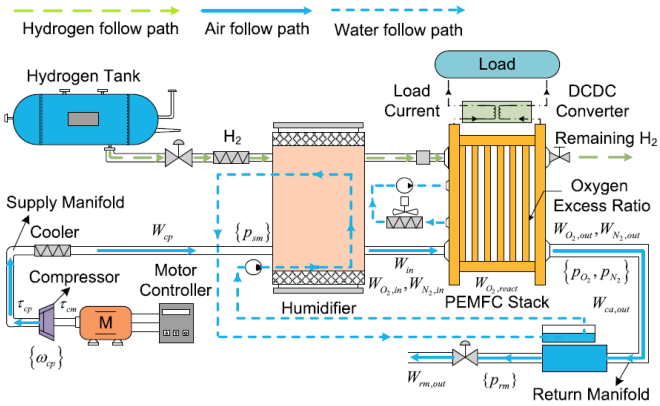

Fig. 1. Structure of the fuel cell system adopted from [10].

The focus of this research paper among the FC system components is the air supply system. Multiple components are part of the air supply system: air compressor, humidifier, air supply manifold, return manifold, and others. The air cooler maintains the temperature of the air entering the stack at 80°C. This assumption is justified because the stack temperature changes relatively slowly.

Additionally, it is assumed that the temperature and humidity of the reactant flows are precisely controlled, which could be achieved through the implementation of effective humidity and cooling subsystems. Models for the FC stack, compressor, and manifolds are presented in the following sections.

A. Stack Voltage Model

The voltage model contains an equation to calculate stack voltage based on FC pressure, temperature, reactant gas partial pressures and membrane humidity. The dynamically varying pressure and relative humidity of the reactant gas flow inside the stack flow channels are calculated in the cathode and the anode flow models.

The output voltage of a PEMFC can be calculated by subtracting the overpotential caused by all polarization phenomena from the reversible voltage. Hence, the output voltage of a FC can be expressed as:

$$v_{fc} = E_{nernst} - v_{act} - v_{ohmic} - v_{conc} \tag{1}$$

where E_{nernst} is the reversible voltage, v_{act} is the activation overvoltage, v_{ohmic} is the ohmic overvoltage, and v_{conc} is the concentration difference over voltage, they are calculated as follows:

$$E_{nernst} = 1.229 - 8.5 \times 10^{-4}\left(T_{fc} - 298.15\right) + 4.308 \times 10^{-5} T_{fc}\left[ln\frac{p_{H_2}}{1.01325} + 0.5 ln\frac{p_{O_2}}{1.01325}\right] \tag{2}$$

$$v_{act} = v_0 + v_a(1 - e^{-c_1 i}) \tag{3}$$

$$v_{ohmic} = i.R_{ohmic} \tag{4}$$

$$v_{conc} = i\left(c_2 \frac{i}{i_{max}}\right)^{c_3} \tag{5}$$

The stack voltage is calculated as a function of stack current, cathode pressure, reactant partial pressures, FC temperature and membrane humidity. Detailed explanations for the equations can be found in [11]. The stack voltage can be determined by multiplying the individual cell voltage, v_{fc}, by the total number of cells, n, in the stack.

$$v_{st} = n \times v_{fc} \tag{6}$$

Hence, the total output power of PEMFC power generation system is the product of stack current and voltage:

$$P_{st} = v_{st} \times I_{st} \tag{7}$$

B. Air Compressor Model

The system mainly interfaces with the atmospheric environment using the air compressor. The model takes in the control voltage and altitude as inputs and generates the inlet flow of the supply manifold as output. The dynamic behavior of the compressor speed can be calculated as follow [11]:

$$J_{cp}\frac{d\omega_{cp}}{dt} = \left(\tau_{cm} - \tau_{cp}\right) \tag{8}$$

where ω_{cp} is the angular velocity of the air compressor, J_{cp} is the moment of inertia, τ_{cm} is the compressor motor torque, τ_{cp} is the torque required to drive the compressor.

The compressor motor torque is calculated using a static motor equation:

$$\tau_{cm} = \eta_{cm}\frac{k_t}{R_{cm}}\left(v_{cm} - k_v\omega_{cp}\right) \tag{9}$$

where k_t, R_{cm}, and k_v are motor constants and η_{cm} is the motor mechanical efficiency. The values are given in TABLE I [11].

TABLE I. COMPRESSOR PARAMETERS

Parameter	Value	Unit
k_v	0.0153	$V/(rad/sec)$
k_t	0.0153	$N-m/Amp$
R_{cm}	0.82	Ω
η_{cm}	98%	-

The torque required to drive the compressor is calculated using the thermodynamic equation:

$$\tau_{cp} = \frac{C_p}{\omega_{cp}}\frac{T_{atm}}{\eta_{cp}}\left[\left(\frac{p_{sm}}{p_{atm}}\right)^{\frac{\gamma-1}{\gamma}} - 1\right]W_{cp} \tag{10}$$

Where, C_p is the air specific heat capacity, T_{atm} is the air temperature at the inlet of compressor, γ is the air specific heat ratio, η_{cp} is the efficiency of compressor.

To obtain the air flow rate through the compressor, W_{cp}, a static compressor map is used, and the compressor flow characteristic is modeled by the Jensen and Kristensen nonlinear curve fitting method [12]. The compressor characteristics are given in [11].

C. Supply Manifold Model

The cathode supply manifold includes an assembly of pipes and manifold volumes connecting the air compressor to the stack cathode. The pressure within the supply manifold, p_{sm}, is determined by applying equations based on mass continuity and energy conservation [13].

$$\frac{dm_{sm}}{dt} = W_{cp} - W_{sm,out} \tag{11}$$

$$\frac{dp_{sm}}{dt} = \frac{\gamma R_a}{V_{sm}}\left(W_{cp}T_{cp,out} - W_{sm,out}T_{sm}\right) \tag{12}$$

where R_a is the air gas constant, V_{sm} is the supply manifold volume, and T_{sm} is the temperature of the flow inside the manifold calculated from the ideal gas law. The supply manifold exit flow, $W_{sm,out}$, is calculated as a function of p_{sm} and p_{ca} using the linearized nozzle flow equation. In this equation $k_{sm,out}$ is the supply manifold outlet flow constant.

$$W_{sm,out} = k_{sm,out}(p_{sm} - p_{ca}) \tag{13}$$

D. Return Manifold Model

Due to the comparatively low temperature of the air exiting the stack, the air temperature within the return manifold, T_{rm} , is consequently considered constant and equal to the stack temperature. The return manifold pressure, p_{rm} , is modeled using the mass conservation and the ideal gas law [13].

$$\frac{dp_{rm}}{dt} = \frac{R_a T_{rm}}{V_{rm}}\left(W_{ca,out} - W_{rm,out}\right) \tag{14}$$

E. Cathode Flow Model

This model captures the cathode air flow behavior. To achieve a dynamic mass balance in the cathode channel, it is essential to consider the thermodynamic properties and mass conversion law of oxygen, nitrogen, and water vapor. Then, the dynamics of the gas in the cathode is given by the following formula according to the principle of mass flow continuity:

$$\frac{dm_{O_2,ca}}{dt} = W_{O_2,ca,in} - W_{O_2,ca,out} - W_{O_2,reacted} \tag{15}$$

$$\frac{dm_{N_2,ca}}{dt} = W_{N_2,ca,in} - W_{N_2,ca,out} \tag{16}$$

$$\frac{dm_{w,ca}}{dt} = W_{v,ca,in} - W_{v,ca,out} + W_{v,ca,gen} + W_{membr} - W_{l,ca,out} \tag{17}$$

Where, $W_{O_2,ca,in}$ and $W_{O_2,ca,out}$ are the mass flow of oxygen into and out of the cathode; $W_{N_2,ca,in}$ and $W_{N_2,ca,out}$ are the mass flow of nitrogen into and out of the cathode; $W_{v,ca,in}$ and $W_{v,ca,out}$ are the mass flow rates of water vapor entering and exiting the cathode; $W_{O_2,reacted}$ and $W_{v,ca,gen}$ are the mass flow of oxygen consumed by the reaction and the mass flow of water vapor generated; $W_{v,membr}$ is the mass flow of water conducted from the anode to the cathode; $W_{l,ca,out}$ is the mass flow of water flowing out of the cathode in the form of liquid, which is generally taken as 0.

F. Anode Flow Model

This model is quite like the cathode flow model. Hydrogen partial pressure and anode flow humidity are determined by balancing the mass of hydrogen, $m_{H_2,an}$, and water in the anode, $m_{w,an}$.

$$\frac{dm_{H_2,an}}{dt} = W_{H_2,an,in} - W_{H_2,an,out} - W_{H_2,reacted} \tag{18}$$

$$\frac{dm_{w,an}}{dt} = W_{v,an,in} - W_{v,an,out} - W_{v,membr} - W_{l,an,out} \tag{19}$$

Here, pure hydrogen gas is assumed to be supplied to the anode from a hydrogen tank. Also, it is assumed that the hydrogen flow rate can be instantly adjusted by a valve while maintaining a minimum pressure difference across the membrane.

III. Steady State Analysis

In this section, the optimal steady-state operating point for the air compressor is studied. The net power of the FC system, P_{net}, which is the difference between the power produced by the stack, P_{st} , and the parasitic power, should be maximized.

$$P_{net}(I_{st}, \upsilon_{cm}) = P_{st}(I_{st}) - P_{compressor} \tag{20}$$

$$P_{compressor} = \frac{C_p T_{atm}}{\eta_c}\left[\left(\frac{p_{atm}}{p_{sm}}\right)^{\frac{1-\gamma}{\gamma}} - 1\right]W_{cp} \tag{21}$$

Most of the parasitic power for a FC system is spent on the air compressor; thus, it is important to determine the proper air flow [14]. The air flow excess is reflected by the term OER, λ_{O_2}, defined as the ratio of oxygen supplied to oxygen used in the cathode, that is,

$$\lambda_{O_2} = \frac{W_{O_2,ca,in}}{W_{O_2,reacted}} \tag{22}$$

Increasing the OER initially results in higher oxygen partial pressure, leading to improvements in P_{st} and P_{net}. However, once the optimal value is reached, further increases in OER would result in only marginal increases in P_{st}, and an increase in compressor power consumption, causing a decrease in P_{net}.

To identify the optimal value for OER, the model is executed repeatedly, and steady-state values of OER and P_{net} at different stack current, is plotted (Fig. 2). The optimal OER varies between 2.0 and 2.4 and decreases slowly when the stack current increases. It should be noted that to enhance the readability, the graph displays results for currents ranging from 100 to 280 amps, with 20-amp intervals, whereas the calculations cover a range from 1 to 280 amps at 1-amp intervals.

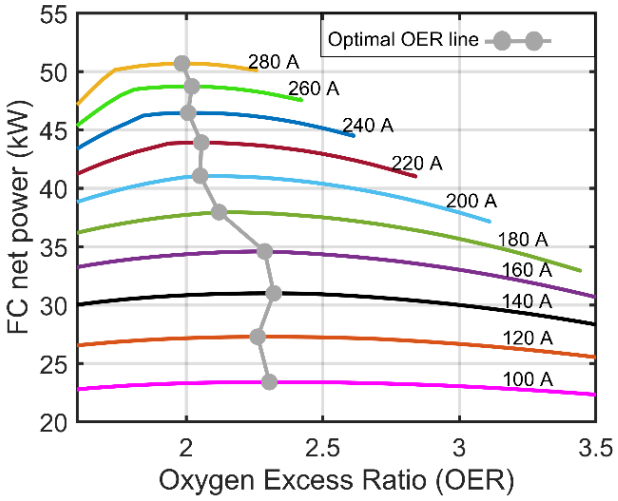

Fig. 2. System net power at different stack current and oxygen excess ratios

IV. Energy Management Strategy

The performance of a hybrid FC system is investigated with a variable OER. The energy management strategy is optimization-based. More specifically, sequential quadratic programming (SQP) is an online strategy that does not require a priori knowledge of the driving cycle. This strategy illustrates the influence of the optimal OER tracking over the hydrogen consumption of the hybrid FC system.

The power demand (P_{req}) from the electric motor side is supplied by both of PEMFC and battery pack. Therefore, the fuel economy of a hybrid FC system relies on how the requested power is distributed between these two sources.

$$P_{req} = \eta_{DC-DC} P_{net} + P_{Bat} \tag{23}$$

In this study, the goal of the EMS is to determine an online power split trajectory that minimizes hydrogen consumption in the PEMFC while adhering to the system's constraints. The hydrogen consumption of the system is expressed as follows:

$$H_2\left(P_{FC,t}\right) = a_1 P_{st,t}^2 + a_2 P_{st,t} + a_3 \tag{24}$$

To ensure that the power sources operate within acceptable limits, the EMS incorporates the following constraints.

$$\begin{cases} P_{st,min} \le P_{st,t} \le P_{st,max} \\ \qquad (P_{st,min} = 0kW, P_{st,max} = 75kW) \\ \Delta P_{st,min} \le P_{st}(t) - P_{st}(t-1) \le \Delta P_{st,max} \\ \qquad (\Delta P_{st,min} = -7.5\ {}^{kW}/_{s},\ \Delta P_{st,max} = 7.5\ {}^{kW}/_{s}) \\ SOC_{min} \le SOC(t) \le SOC_{max} \\ \qquad (SOC_{min} = 50\%, SOC_{max} = 90\%) \\ P_{bat,min} \le P_{bat,t} \le P_{bat,max} \\ \qquad (P_{bat,min} = -30kW, P_{bat,max} = 40kW) \end{cases} \tag{25}$$

Where $P_{st,min}$, $P_{st,max}$, $\Delta P_{st,min}$, $\Delta P_{st,max}$, SOC_{min}, SOC_{max}, $P_{bat,min}$, and $P_{bat,max}$ are minimum and maximum values of FC stack power, FC stack power variation, battery SOC, and battery power.

V. Results and Discussion

The results obtained in this work are provided in this section. The performance of the formulated EMS is explored under the presented mission profile in Fig. 3.

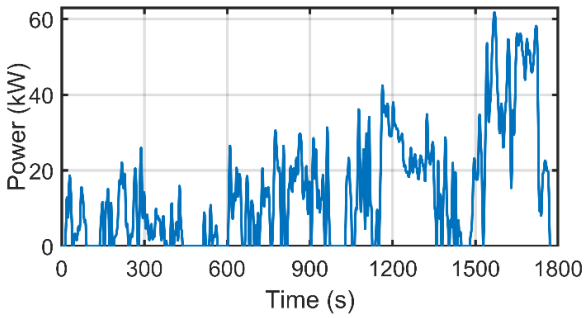

Fig. 3. WLTC Class 3 driving cycle

The EMS is examined by considering two cases. First, constant OER: the required power from the PEMFC is determined by EMS while the OER is assumed to be constant and equal to 2. Second, EMS using optimum OER: this scenario investigates the performance of the strategy while utilizing optimal OER.

Fig. 4 shows the performance of the EMS. Fig. 4a shows the share of net power that the FC should supply, while Fig. 4b presents the power provided by the battery. It is evident that the battery absorbs sudden peaks to prevent any starvations in the FC system. Fig. 4c indicates the variation of the battery SOC, starting with an initial value of 70% and ending at almost 68%.

Fig. 5 compares the gross stack power required by the FC to meet the net power demand in each case study of constant and optimal OER. This figure reveals that with a constant OER, the gross stack power is higher compared to when the optimal OER is used. This difference becomes more pronounced in the mid-operating range of the FC system, specifically from 1200 s to approximately 1350 s. In this interval, the disparity between the optimal OER and the tested constant OER is significantly larger. The difference becomes less significant from 1550 to nearly 1750 seconds, as shown in Fig. 5, due to the minimal variance between the optimal and constant OER values in this interval. It is important to highlight that both methods attained the same FC net power.

To quantify the extent of this difference between the two case studies, the total hydrogen consumption, a direct result of the gross stack power, is reported in Fig. 6. According to this figure, the use of optimal OER led to a consumption of approximately 350 g of hydrogen, while the constant OER resulted in more than 360 g. This indicates that the use of optimal OER has led to an almost 3% reduction in hydrogen consumption in the conducted study.

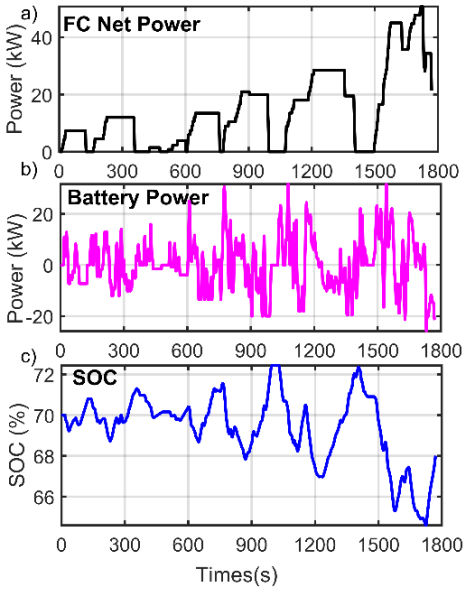

Fig. 4. The obtained FC net power (a), battery power (b) and battery SOC (c) using the designed EMS.

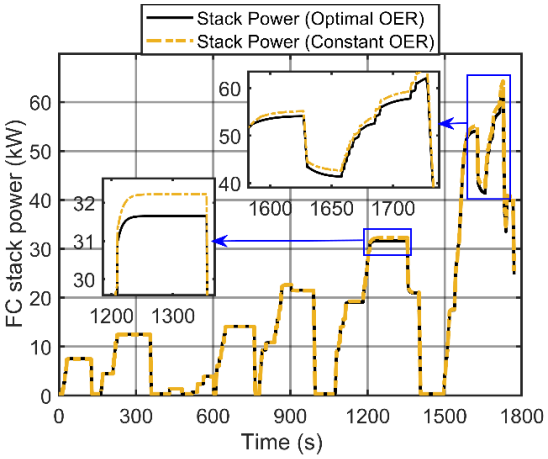

Fig. 5. Gross fuel cell stack power for the two case studies.

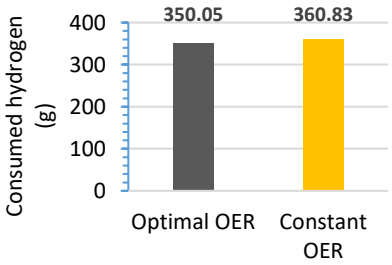

Fig. 6. Hydrogen consumption of each performed case study.

VI. Conclusion

This paper investigates the influence of optimal OER tracking over the hydrogen consumption of a hybrid FC system. In this respect, an optimization-based EMS is formulated for hydrogen consumption minimization of a PEMFC stack. Similar to the existing EMSs in the literature, the EMS determines the required net power from the PEMFC stack, while respecting the limitation of the power sources, and the remainder is supplied by the battery pack. Results show that following the optimal trajectory of OER would decrease the hydrogen consumption around 3% for a standard mission profile at sea level conditions.

Acknowledgment

The authors would like to thank the Natural Science and Engineering Research Council of Canada, CRIAQ (Consortium de recherche et d'innovation en aérospatiale au Québec), Flying Whales, Pratt & Whitney Canada, and MTLS-Aero Structure.

References

[1] F. Ülengin, M. Işık, Ş. Ö. Ekici, Ö. Özaydın, Ö. Kabak, and Y. İ. Topçu, "Policy developments for the reduction of climate change impacts by the transportation sector," *Transport Policy*, vol. 61, pp. 36-50, 2018.

[2] C. Acar and I. Dincer, "The potential role of hydrogen as a sustainable transportation fuel to combat global warming," *International Journal of Hydrogen Energy*, vol. 45, no. 5, pp. 3396-3406, 2020.

[3] Y. Huang, H. Wang, A. Khajepour, B. Li, J. Ji, K. Zhao, and C. Hu, "A review of power management strategies and component sizing methods for hybrid vehicles," *Renewable and Sustainable Energy Reviews*, vol. 96, pp. 132-144, 2018.

[4] S. Li, Y. Qiu, L. Yin, R. Li, R. Gan, Q. Li, and Y. Huangfu, "Net power optimization based on extremum search and model-free adaptive control of PEMFC power generation system for high altitude," *IEEE Transactions on Transportation Electrification*, 2022.

[5] Q. Shen, M. Hou, X. Yan, D. Liang, Z. Zang, L. Hao, Z. Shao, Z. Hou, P. Ming, and B. Yi, "The voltage characteristics of proton exchange membrane fuel cell (PEMFC) under steady and transient states," *Journal of Power Sources*, vol. 179, no. 1, pp. 292-296, 2008.

[6] C. A. Ramos-Paja, R. Giral, L. Martinez-Salamero, J. Romano, A. Romero, and G. Spagnuolo, "A PEM fuel-cell model featuring oxygen-excess-ratio estimation and power-electronics interaction," *IEEE Transactions on Industrial Electronics*, vol. 57, no. 6, pp. 1914-1924, 2009.

[7] M. Kandidayeni, A. Macias, L. Boulon, and S. Kelouwani, "Investigating the impact of ageing and thermal management of a fuel cell system on energy management strategies," *Applied Energy*, vol. 274, p. 115293, 2020.

[8] N. Sulaiman, M. Hannan, A. Mohamed, P. J. Ker, E. Majlan, and W. W. Daud, "Optimization of energy management system for fuel-cell hybrid electric vehicles: Issues and recommendations," *Applied energy*, vol. 228, pp. 2061-2079, 2018.

[9] M. Kandidayeni, A. Macias, L. Boulon, and S. Kelouwani, "Efficiency upgrade of hybrid fuel cell vehicles' energy management strategies by online systemic management of fuel cell," *IEEE Transactions on Industrial Electronics*, vol. 68, no. 6, pp. 4941-4953, 2020.

[10] Y. Wang and Y. Wang, "Pressure and oxygen excess ratio control of PEMFC air management system based on neural network and prescribed performance," *Engineering Applications of Artificial Intelligence*, vol. 121, p. 105850, 2023.

[11] J. T. Pukrushpan, H. Peng, and A. G. Stefanopoulou, "Control-oriented modeling and analysis for automotive fuel cell systems," *J. Dyn. Sys., Meas., Control*, vol. 126, no. 1, pp. 14-25, 2004.

[12] P. Moraal and I. Kolmanovsky, "Turbocharger modeling for automotive control applications," SAE Technical Paper, 0148-7191, 1999.

[13] H. Deng, Q. Li, Y. Cui, Y. Zhu, and W. Chen, "Nonlinear controller design based on cascade adaptive sliding mode control for PEM fuel cell air supply systems," *International Journal of Hydrogen Energy*, vol. 44, no. 35, pp. 19357-19369, 2019.

[14] J. Chen, Z. Liu, F. Wang, Q. Ouyang, and H. Su, "Optimal oxygen excess ratio control for PEM fuel cells," *IEEE Transactions on control systems technology*, vol. 26, no. 5, pp. 1711-1721, 2017.